J Mater Sci: Mater Med (2010) 21:2115–2124
DOI 10.1007/s10856-010-4072-y

Fiber scaffolds of polysialic acid via electrospinning for peripheral nerve regeneration

Ulrike Assmann · Andreas Szentivanyi · Yvonne Stark · Thomas Scheper · Silke Berski · Gerald Dräger · Robert H. Schuster

Received: 25 September 2009 / Accepted: 22 March 2010 / Published online: 9 June 2010

Abstract Fiber scaffolds of bioactive polysialic acid have been prepared via electrospinning for peripheral nerve regeneration. The diameter, morphology and alignment of fibers in scaffolds were adjusted by variation of electrospinning parameters, which are decisive for the cell-scaffold interaction. Due to the high water solubility of polysialic acid (poly-α-2,8-*N*-acetylneuraminic acid) a photoactive derivative (poly-α-2,8-*N*-pentenoylneuraminic acid) was used to obtain stable fiber scaffolds in water by photochemical crosslinking. At the optimized fiber scaffolds good cell viability and directed cell proliferation along the fibers was achieved by cell tests with immortalized Schwann cells.

1 Introduction

The goal of tissue engineering is to create a living construct with the ability to mimic the complexities of tissue functions. Engineered tissues consist of cells and scaffold, which substitute the native extracellular matrix (ECM). In native tissue cells interact constantly with the ECM and it guides their proliferation [1]. Therefore scaffolds have to meet various requirements like mechanical stability, biocompatibility and nanoscale topography [2]. Scaffolds with these requirements can be prepared via electrospinning by creating a nano scaled fiber scaffold similar like the three-dimensional network structure of collagen multi-fibrils (50–500 nm) with proteoglycans in native ECM [3]. Due to the high flexibility of the electrospinning process, suitable materials and additional additives can be selected to adjust the fiber properties for specific cell types [4, 5].

Peripheral nerve injuries occur several hundred thousand times each year in Europe and the US alone [6, 7]. Aligned fiber scaffolds help guide the naturally regenerating axons from the proximal stump to the distal segment of the injured nerve to finally restore function and disfigurement. Polymers like poly-ε-caprolactone [8], poly(L-lactic acid) [9] and poly(L-lactide-*co*-glycolide) [10] were already investigated as neural fiber scaffold.

In current investigations polysialic acid (poly-α-2,8-*N*-acetylneuraminic acid, PSA) plays a decisive role for peripheral nerve regeneration [11]. PSA is an alpha-2,8-linked polysaccharide (Fig. 1), which is highly hydrophilic due to its carboxylic function.

In the brain and in the central nerve system of vertebrates, PSA occurs in high amount during embryonic development. During the growth process PSA regulates the function of the neural cell adhesion molecules (NCAM) [12]. Thereby PSA plays an important part in cell migration, axonal guidance, synapse formation, and functional plasticity of the nervous system [13] as well as tumor progression and differentiation [14].

The goal of this work is to combine the bioactivity of PSA with the nanoscale topography of electrospun fibers to

U. Assmann · R. H. Schuster (✉)
Deutsches Institut für Kautschuktechnologie e.V., Eupener Straße 33, 30519 Hannover, Germany
e-mail: Robert.Schuster@dikautschuk.de

A. Szentivanyi
Institut für Mehrphasenprozesse, Universität Hannover, Hannover, Germany

Y. Stark · T. Scheper
Institut für Technische Chemie, Universität Hannover, Hannover, Germany

S. Berski · G. Dräger
Institut für Organische Chemie, Universität Hannover, Hannover, Germany

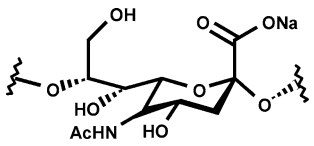

Fig. 1 Poly-α-2,8-*N*-acetylneuraminic acid (PSA)

obtain a bio-identical scaffold for peripheral nerve regeneration.

To achieve this goal, the binary polymer system, PSA with polyethylene oxide (PEO), was electrospun. After electrospinning the water soluble PSA/PEO fibers had to be crosslinked to achieve stable fiber scaffolds for cell tests. Recently, it has been shown that PEO can successfully be crosslinked by irradiation with ultraviolet (UV) light using benzophenone as photoinitiator [14]. Based on this knowledge, a photoactive derivate (poly-α-2,8-*N*-pentenoylneuraminic acid, PEN) was used besides PSA as scaffold material.

The work is divided as follows: (1) characterization of the photoactive derivative, PEN, (2) investigation of the electrospinning process with regard to the morphology and the diameter of the fibers, (3) cross-linking of the fibers to reduce the water solubility and finally (4) in vitro cell tests to investigate proliferation and viability of Schwann cells on the fiber scaffolds.

2 Materials and methods

2.1 Materials

PSA (Mw: 30.000 g/mol) was delivered by Nacalai and converted to poly-α-2,8-*N*-pentenoylneuraminic acid (PEN). The polyethylene oxide PEO (Mw: 600.000 g/mol) and the ethanol (p.a.) were delivered by Fluka. For crosslinking the fibers a triacrylate (trimethylpropane ethoxylate triacrylate) from Aldrich and the photoinitiator (Irgacure® 500), a mixture of 1-hydroxy-cyclohexyl-phenyl-ketone and benzophenone, from Ciba were used.

2.2 Characterization methods

Infrared (IR) spectra of the derivates and fiber scaffolds were measured with a Thermo Nicolet Nexus spectrometer in ATR (Attenuated Total Reflection) mode with a diamond crystal. The water based eluate of the fiber scaffold was transferred by a reversed phase column (Bakerbond® C_{18}, 40 µm Prep LC Packing, J.T. Baker) in an organic phase of methanol and dichloromethane for IR measurements in transmission mode, using a barium fluoride crystal.

The solubility of PSA and PEN in a water:ethanol mixture was measured by a turbidity measurement. They were precipitated by gradual addition of ethanol in the water based solution. The precipitation point was determined by measuring the scattering of a laser beam (wavelength: 632.8 nm) with a silicon photodiode, which goes directly through the solution.

The viscosity, conductivity and surface tension of the polymer solution were measured at room temperature by a rheometer (Rheometrics Fluid Spectrometer, plate-plate, shear rate between 47 and 52 s^{-1}), a conductometer (Metrohm) and a tensiometer (Dataphysics, Wihelmy plate).

Morphology and diameter of the fibers were measured by a transmission electron microscope TEM (LIBRA 120, Zeiss) and an atomic force microscope AFM (Topometrix Explorer 2000). A copper grid (200 mesh) for TEM and a glass slide for AFM measurements were used as sample carrier.

2.3 Electrospinning

The fundamental component of an electrospinning setup (Fig. 2) is the high voltage power supply (Matsusada, AU-50P2-L), which is connected to a nozzle. The polymer solution runs out of the nozzle with a constant flow rate, which can be adjusted by a syringe pump (Syringe pump, NE-500 OEM). The nozzle consists of a steel capillary with an inner diameter of 0.8 mm. The fibers are collected on a microscope slide above the grounded counter electrode.

In this study all fiber scaffolds were produced at an electrode distance of 20 cm, an applied voltage of 5.5 kV and a flow rate of 0.02 ml/h.

2.4 Photocrosslinking

Triacrylate (15 mg/ml) and photo initiator (5 mg/ml) were added to the PSA/PEN (6.7 mg/ml) and PEO (26.8 mg/ml) solution. The fibers were electrospun from a water:ethanol (1:1) solution and dried at 35°C for 14 h. Under nitrogen the fibers were crosslinked with a UV light source (Minerallight® Lamp, UVGL-58, 115 W) at a wavelength of 366 nm. Fibers without PSA/PEN were produced as

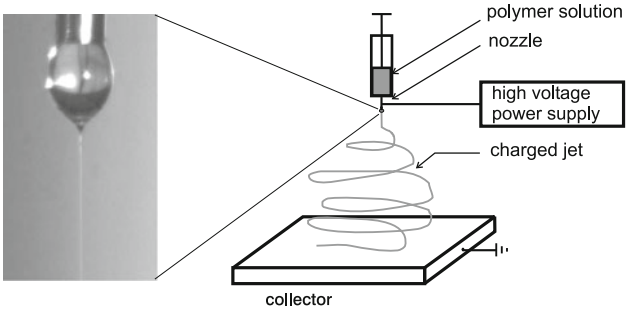

Fig. 2 Electrospinning set-up

reference. The fiber scaffolds were treated with water for 24 h after crosslinking to check their stability.

2.5 Cell culture

2.5.1 MTT assay

In vitro experiments were performed with immortalized Schwann cells, which are used as neuronal cell model. The fibers were electrospun on glass slides, which had previously been disinfected with a 70% isopropanol, brought into tissue culture vials and pre-incubated with medium over-night. The medium was carefully removed and the samples were incubated in 40 µl cell suspension (75,000 cells/ml). After cell attachment on the material (1.5 h) the medium was filled up. After 6 days the cell viability was measured by a MTT (3-(4,5-dimethylthiazol-2-yl)-2,5-diphenyltetrazoliumbromid) assay. Each experiment was performed 6 times in parallel. 100 µl of culture medium and 10 µl of MTT solution (5 mg/ml phosphate buffered saline PBS, sterile filtrated) were added to each well and incubated for 4 h at 37°C and 5% CO_2. Afterwards, 100 µl of 10% sodium dodecyl sulfate SDS (w/v) in 0.01 M HCl was added and the samples were incubated for 24 h. The transmission signal at 570/630 nm was measured using a microplate reader (Bio-Rad, Munich, Germany). A glass slide without cells was used as a baseline value. The data were presented as the mean values standard deviation of six replicates for each sample. Variances within each group were calculated using the f test. Statistical significance was considered for $P < 0.05$.

2.5.2 DAPI staining

In order to visualize the cells on the glass slides, double-stranded DNA of the cell nuclei was stained by histological staining with 40,6-diamidino-2-phenylindole dihydrochloride (DAPI). Each experiment was performed 6 times in parallel in a 96-well culture plate. After 6 days, the cultivation glass slides were washed with PBS to remove nonattached cells. Afterwards absolute ethanol (200 ml) was added and the glass slides were stored for 30 min at − 20°C. Then the cells were washed twice with PBS and the cell nuclei were stained by addition of 200 µl of DAPI-staining solution (2 µl of DAPI-stock solution in 1 ml of buffer). The slides were incubated at 37°C for 20 min and subsequently washed 3 times with PBS. Afterwards the glass slides were observed with UV light using a fluorescence microscope. Six images (magnification ×400) of each slide were taken. After 6 days of cultivation on the glass slides analogue to viability assay and cell morphology were examined.

3 Results

3.1 Characterization of PEN

Poly-α-2,8-*N*-pentenoylneuraminic acid (PEN) was prepared using poly-α-2,8-*N*-acetylneuraminic acid as starting material and characterized by ^{1}H- and ^{13}C-NMR.

The infrared spectra show a band drift of the amide to lower wave numbers from 1,565 to 1,555 cm^{-1}. In the infrared spectrum of PEN a band of the methylene group at 917 cm^{-1} appears and the CH_3 deformation vibration of the amide at 1,376 cm^{-1} is superposed by a CH_2 vibration at 1,395 cm^{-1} (Fig. 3).

The infrared spectra as well as GCMS show that PSA can be converted to PEN quantitative.

3.2 Influence of process parameters

The electrospinning process is based on electrostatic forces, which stretch a polymer solution during solidification. High voltage is applied to the polymer solution droplet inducing thusly electrical charges. Due to the Coulomb repulsion between the induced charges and also due to the external electric field, the droplet is stretched until the electrostatic force overcomes the surface tension of the droplet, at this point a thin jet is ejected out of the droplet. The jet is accelerated by the external electric field in the direction of the counter electrode, where the fiber web is collected on a substrate.

Parameters, which influence the electrospinning process, can be divided in solution and process parameters. Important solution parameters are surface tension, conductivity and viscosity, which are connected to the concentration, molecular weight and solubility of the polymer as well as the vapor pressure of the solvent. The process parameters are, for instance, applied voltage, flow rate of

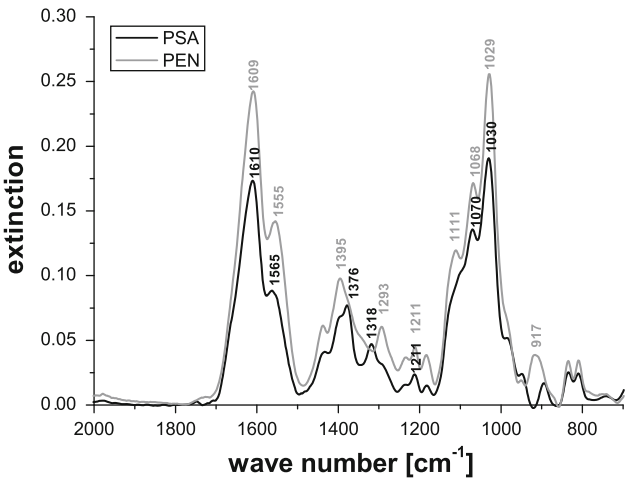

Fig. 3 Infrared spectra of PSA and PEN

the polymer solution, geometry of the electrodes and distance between the electrodes as well as ambient temperature and humidity [16, 17]. With different geometries [18] of the counter electrode, non-woven as well as woven can be collected.

The influence of the main solution parameters, like viscosity, conductivity and surface tension, on morphology and diameter of the fibers were investigated to optimize the topography of the final fiber scaffold for cell tests. For these measurements PSA was used instead of PEN, due to the fact that PSA is easier commercially obtainable, thus higher quantities can be processed. Therefore it was assumed that both polysaccharides, PSA and PEN, have a similar chemical composition, therefore having the same effect on solution parameters like viscosity, conductivity and surface tension.

Before preparing the polymer solutions, turbidity measurements were done to investigate the highest possible PSA/PEN concentrations in a water:ethanol mixture. Thus fiber scaffolds with a high PSA/PEN concentration can be produced to achieve a good bioactivity of the final material. In Fig. 4 the solubility curves of PSA and PEN in water:ethanol as solvent are shown. The PSA solubility is reduced by increasing the ethanol content. PEN is less soluble in a water:ethanol mixture than PSA. The solubility curve has its maximum at an ethanol content of about 0.5. Thus the PSA concentrations and the ethanol content for the polymer solutions (Table 1) were selected from the marked area in Fig. 4.

Due to the low molecular weight of commercial available PSA (Mw: 30.000), no fibers could be spun from pure PSA or PEN solutions. An ideal material to be added to the solution, in order to increase its viscosity and thereby get a stable electrospinning process, was polyethylene oxide (PEO).

Four series of polymer solution were electrospun: the ratio between PSA:PEO and the concentration of polymer

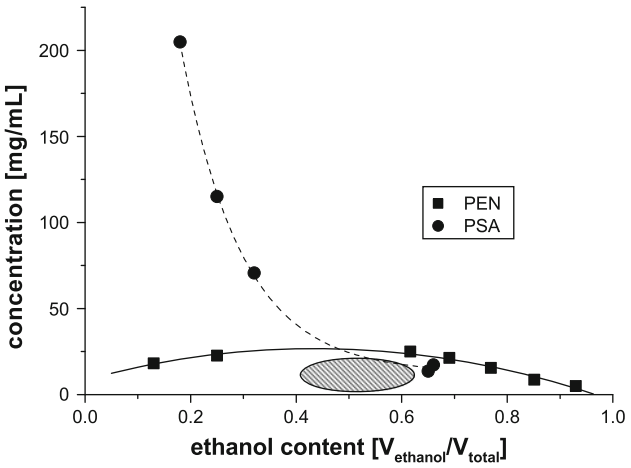

Fig. 4 Solubility curves of PSA and PEN in water:ethanol

Table 1 Overview of characterized polymer solutions

Solution	Polymer (mg/ml)	Mass ratio (m_{PSA}/m_{PEO})	Ethanol content ($V_{ethanol}/V_{total}$)	Variable
1	23	10/13	0.5	PEO ↑
2	27	10/17	0.5	
3	30	10/20	0.5	
4	25	8/17	0.5	PolySia ↑
5	30	13/17	0.5	
6	35	18/17	0.5	
7	33	6.7/27	0.5	PEO + polySia ↑
8	42	8.3/33	0.5	
9	50	10.0/40	0.5	
10	30	13/17	0.66	Solvent ratio
11	30	13/17	0.5	
12	30	13/17	0.33	

as well as ethanol:water were varied therein to investigate the influence of solution parameters like viscosity, conductivity and surface tension on the morphology and diameter of the fibers.

3.2.1 *Polyethylene oxide (PEO) concentration*

In polymer solution 1–3 the PEO concentration was varied. With increasing PEO concentration an increase of the viscosity is detected. The influence on conductivity and surface tension is minor in comparison to the viscosity and can therefore be neglected (Fig. 5a). With the increase in viscosity of the solutions the electrospun fibers show an increase in the fiber diameter (Figs. 5b, 6).

The high molecular weight of PEO (600.000 g/mol) has a strong effect on the viscosity of the solution. The molecular weight influences the entanglement concentration in solution, on which the stability of the jet is depending [19]. By stretching the polymer solution the polymer chains are elongated and partly aligned, which requires a certain amount of force. This strain resistance increases with the viscosity of the polymer solution.

Thus the measurements show that the stretching of the jet between the capillary and the counter electrode is decreased at higher viscosity (Fig. 5b).

3.2.2 *Polysialic acid (PSA) concentration*

In the solutions 4–6 the PSA concentration is varied (Table 1). At higher PSA concentrations the conductivity increase due to fact that PSA is a polyelectrolyte (Fig. 7a), whereas no influence on the viscosity and the surface tension could be detected in this concentration regime.

No significant difference in the average fiber diameter could be caused with increasing conductivity (Fig. 7b). However the fiber morphology is getting smoother with

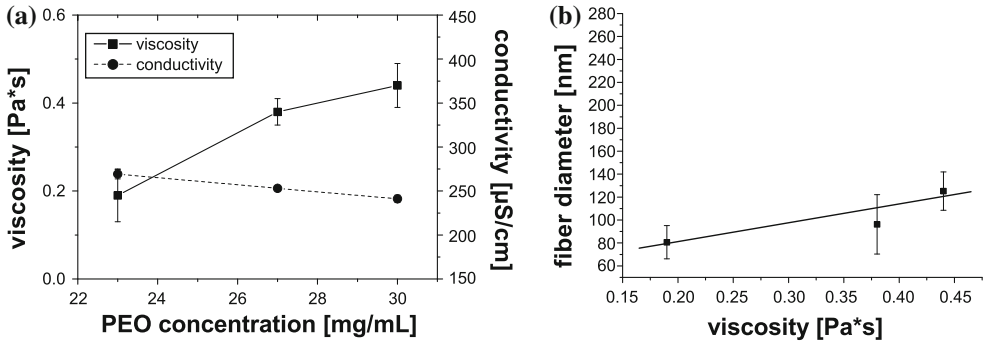

Fig. 5 **a** Influence of the PEO concentration on conductivity and viscosity; **b** fiber diameter at increasing viscosity (see Table 1, polymer solutions 1, 2, 3)

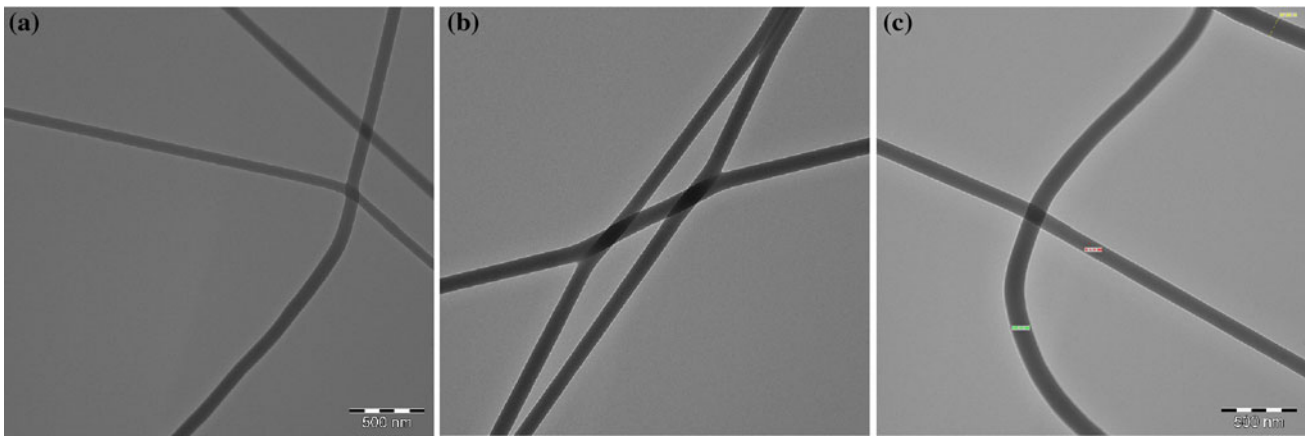

Fig. 6 TEM pictures of nanofibers with different concentrations of PEO (see Table 1, polymer solutions 1, 2, 3)

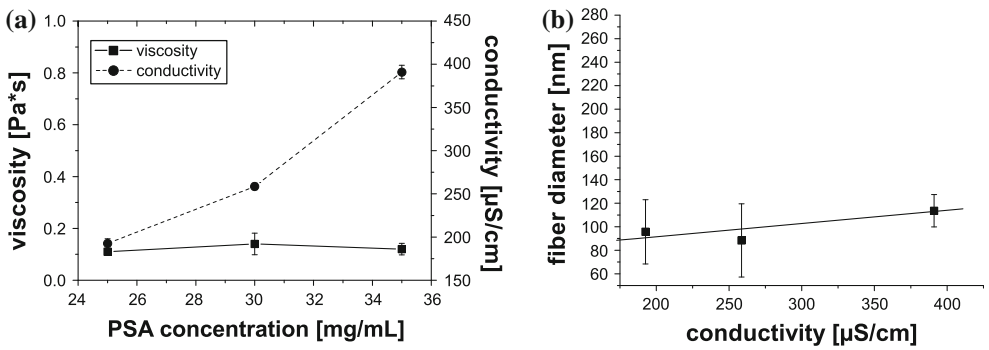

Fig. 7 **a** Influence of the PSA concentration on conductivity and viscosity; **b** fiber diameter at increasing conductivity (see Table 1, polymer solutions 4, 5, 6)

higher PSA concentration as shown in the TEM pictures (Fig. 8). Due to the fact that with higher conductivity the amount of charges per time, carried by the polymer jet from the nozzle to the counter electrode, is increased at a constant applied voltage. With a higher charge density along the jet stronger Coulomb repulsion occurs and increases the instability along the jet, which creates a bending movement [20]. This bending movement induces a stronger stretching of the polymer jet, thus a smoother morphology as well as smaller diameter of the fibers can be obtained [21].

From the described theory it can be concluded that due to stronger stretching of the polymer jet a smoother fiber morphology with increasing PSA concentration could be

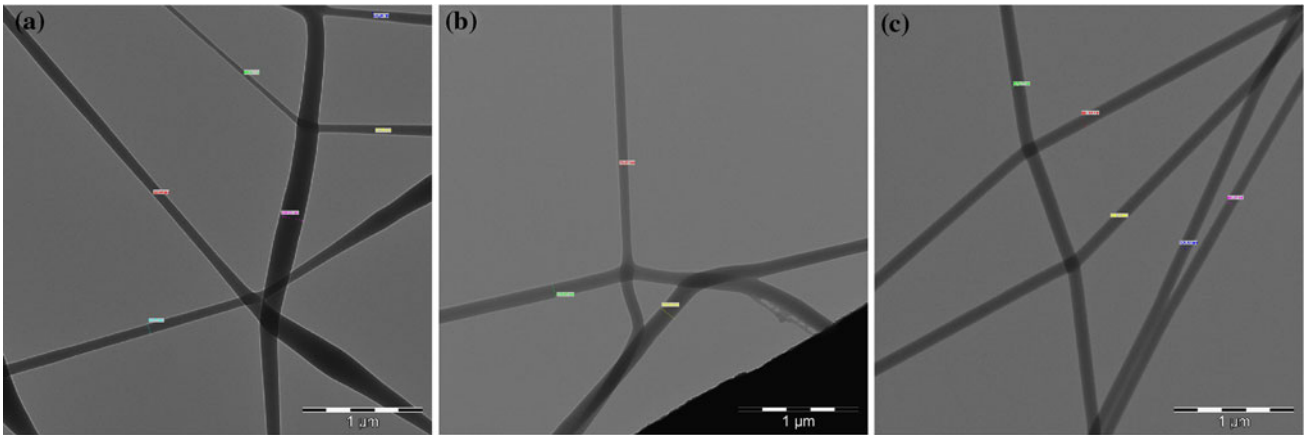

Fig. 8 TEM picture of nanofibers with different PSA concentrations (see Table 1, polymer solution 4, 5, 6)

obtained. Furthermore it can be expected that with a further increase of conductivity the fiber diameter is getting smaller.

3.2.3 Total polymer concentration

In solution 7–9 the ratio between PSA and PEO is kept constant and the total polymer concentration is varied. With the increase of PEO and PSA concentration the viscosity as well as the conductivity increase (Fig. 9a). In Fig. 9b a slight decrease of the fiber diameter as well as of the standard deviation is shown in the first step. By increasing the polymer concentration further the fiber diameter clearly increases.

It can be assumed, that in the first step (solution 8) the polymer jet is more stretched due to the higher conductivity of the polymer solution, which results in a smoother as well as smaller fiber diameter. The same effect is described in the previous series with the PSA concentration (polymer solution 4–6). In the next step at higher polymer concentration (solution 9) the viscosity resistance predominates the stretching along the jet due to the higher conductivity, thus a larger fiber diameter is obtained.

3.2.4 Solvent

By increasing the ethanol content, in the water:ethanol solution, a decrease of the surface tension as well as of the conductivity is noticed (Fig. 11a, b). The influence on the viscosity can be neglected. The electrospun fibers show a clear decrease of the diameter with decreasing ethanol content thus increasing surface tension (Figs. 10, 11c, 12).

Supposedly both parameters, conductivity and surface tension, contribute to the reduction of average fiber diameters with decreasing ethanol content, due to stronger stretching of the polymer jet. The influence of conductivity was already described at the variation of the PSA concentration (solution 4–6). With higher surface tension the critical voltage increases (5.2–5.8 kV), at which the jet is ejected from the droplet on the nozzle [22]. Due to the higher critical voltage more charges are induced and the stretching of the jet by Coulomb repulsion is additionally increased.

After analyzing of the main solution parameters it can be concluded that the variation of the ethanol:water ratio shows the strongest effect on the fiber diameter in comparison to the variation of PSA and PEO concentrations.

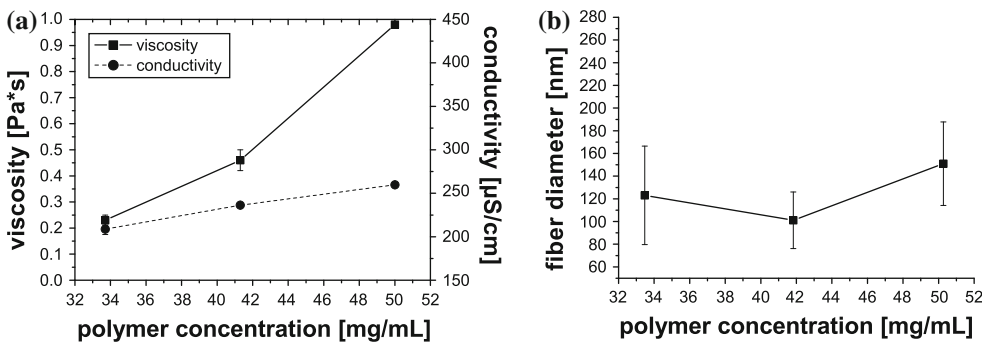

Fig. 9 **a** Influence of the polymer concentration on conductivity and viscosity; **b** fiber diameter at increasing polymer concentration (see Table 1, polymer solutions 7, 8, 9)

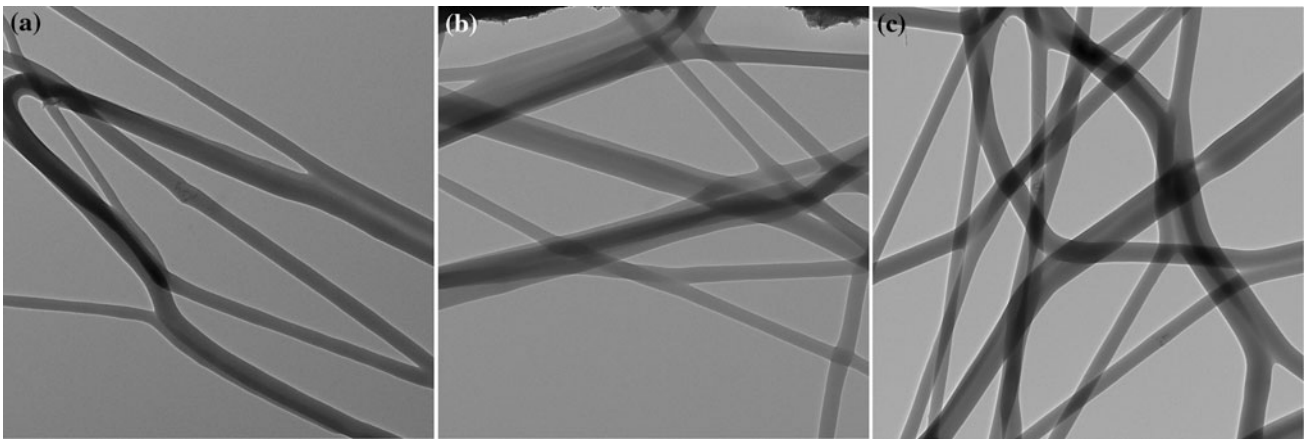

Fig. 10 TEM pictures of nanofibers electrospun at different polymer concentrations (see Table 1, polymer solution 7, 8, 9)

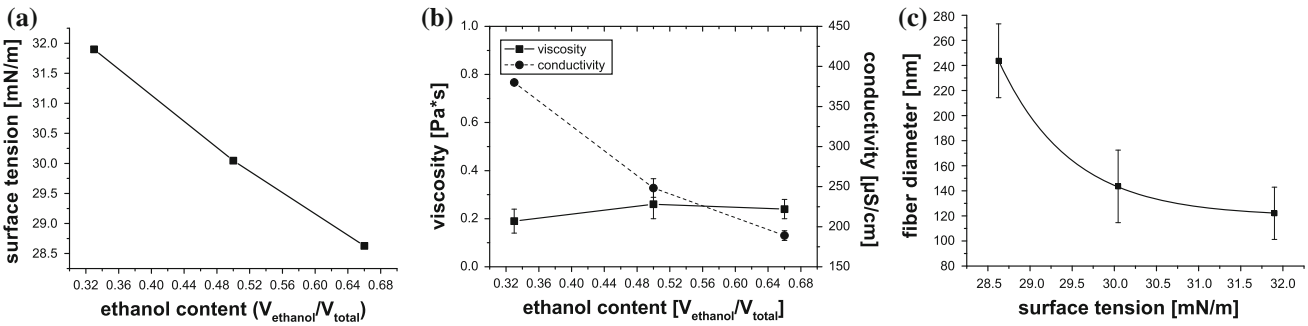

Fig. 11 Influence of the ethanol content **a** on the surface tension, **b** on conductivity and viscosity; **c** fiber diameter at increasing surface tension (see Table 1, polymer solutions 10, 11, 12)

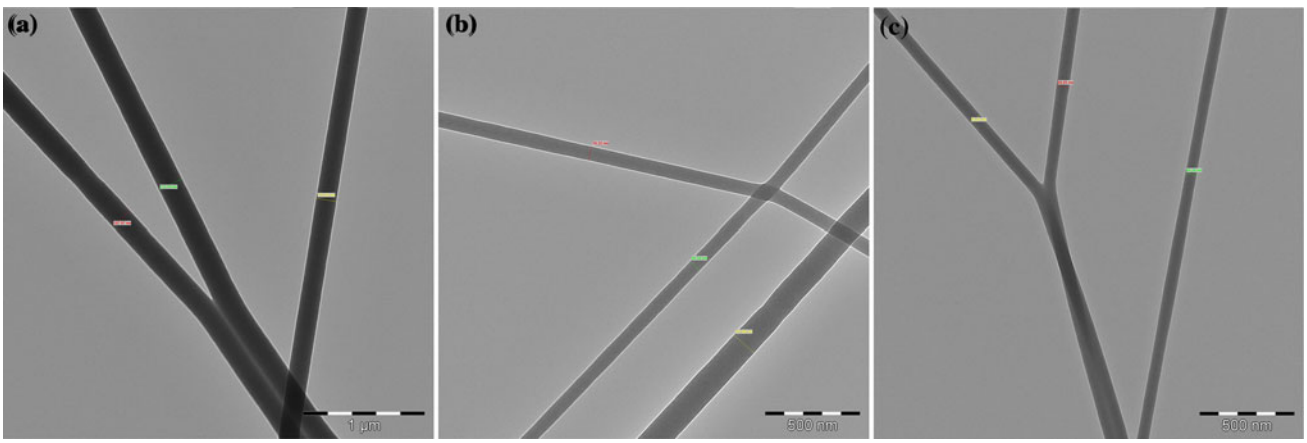

Fig. 12 TEM pictures of nanofibres from polymer solutions (see Table 1, polymer solutions 10, 11, 12) with different solvent ratio (water:ethanol)

With high PEO as well as a high PSA concentration smooth fibers with diameters of about 100–150 nm can be produced, which are similar in size to the collagen fibrils in ECM.

3.2.5 Electrode geometry

The orientation of the fibers is an important factor for scaffolds, especially for peripheral nerve regeneration [23].

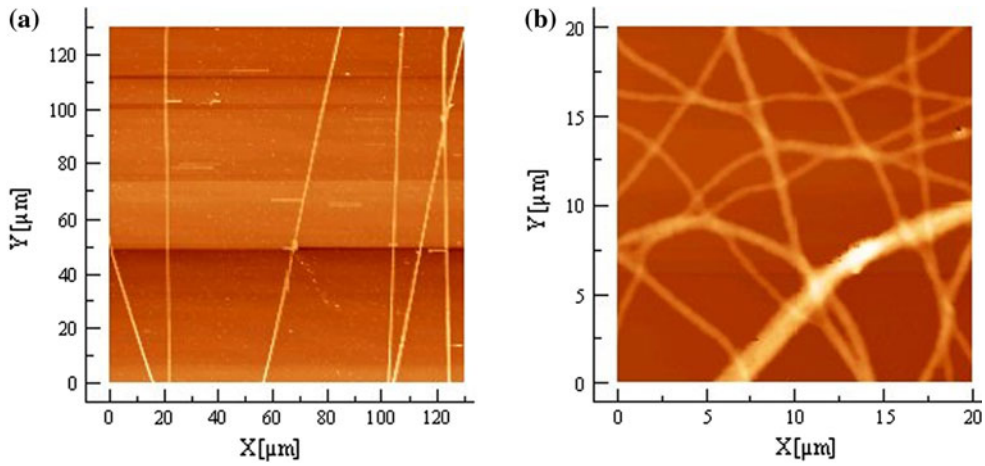

Fig. 13 AFM pictures of nanofibres **a** highly aligned fibres between parallel electrodes **b** non-wovens on top of the electrode

The fiber alignment can be obtained by different techniques. On the one hand a rotating drum can be used to collect the fibers, where the alignment can be adjusted by varying the rotation speed [18]. On the other hand two perpendicular counter electrodes can be used, to receive aligned fibers by horizontal movements between the grounded electrodes. This method is based on the influence on the electric field profile due to the electrode geometry. The electric field lines in the gap near the electrodes are drawn towards their edges. Thus a pulling force is exerted on the electrospinning jet across the gap [24]. Above the electrodes a non-woven and at the same time highly orientated fibers between the electrodes are collected (Fig. 13). A disadvantage is the low density of orientated fibers and the limited electrode distance to guarantee a horizontal movement of the electrospinning jet between the electrodes.

3.3 Crosslinking

After electrospinning the fiber scaffolds were crosslinked by UV radiation and afterwards treated with water for 24 h to investigate the stability in water. In Fig. 14a a comparison between crosslinked fibers with PSA and PEN before and after treatment with water is represented. The acrylate band at 1,732 cm^{-1} is used to standardize the intensity of the spectra in order to compare the intensity of the amide band at 1,610 cm^{-1} of PSA and PEN. As reference the spectrum of the untreated sample of PEN is also shown. The IR spectrum of PSA fibers shows that PSA cannot be detected anymore after 24 h, thus no stabile linkage could be achieved by photochemical crosslinking. The fibers with the photoactive PEN compared to PSA are more stabile in water. The amide band can still be detected after 24 h in water.

In the water extract of the PEN fiber scaffolds different components like PEO (951, 1106, 1246, 1341 cm^{-1}), PEN (1,596 cm^{-1}) and benzophenone (1,279 cm^{-1}) could be detected by infrared spectroscopy (Fig. 14b). These results clearly indicate that the photochemical crosslinking could be improved by using the photoactive PEN instead of PSA.

3.4 Cell tests

After 6 days cultivation of the cells on the glass slides microscopy phase contrast images were performed. The cell

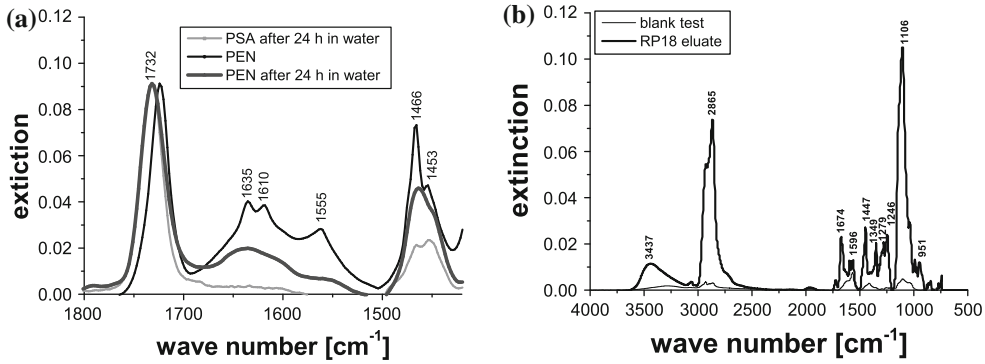

Fig. 14 **a** Infrared spectra of cross-linked fibers before and after treatment with water (24 h); **b** infrared spectrum of extractable components of cross-linked PEN fibers

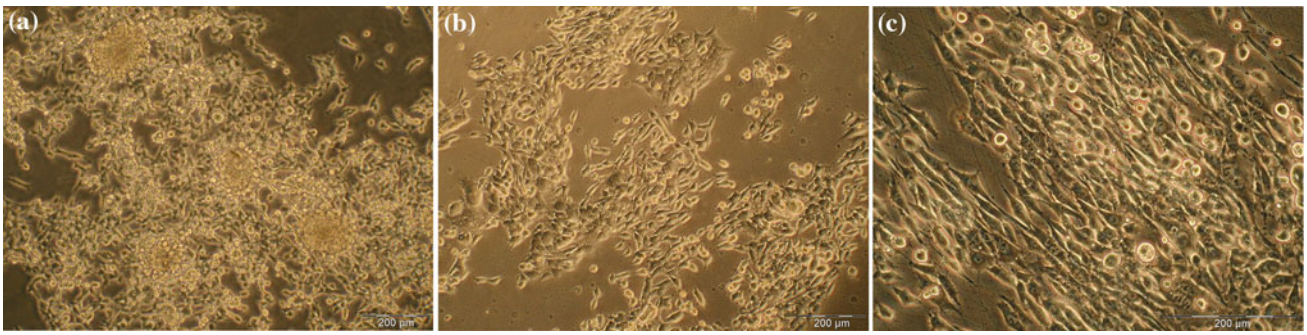

Fig. 15 Phase-contrast pictures of immortalized Schwann cells after 6 days of cultivation; glass slides **a** without fibers, **b** PEO fibers without PEN, **c** PEN fibers

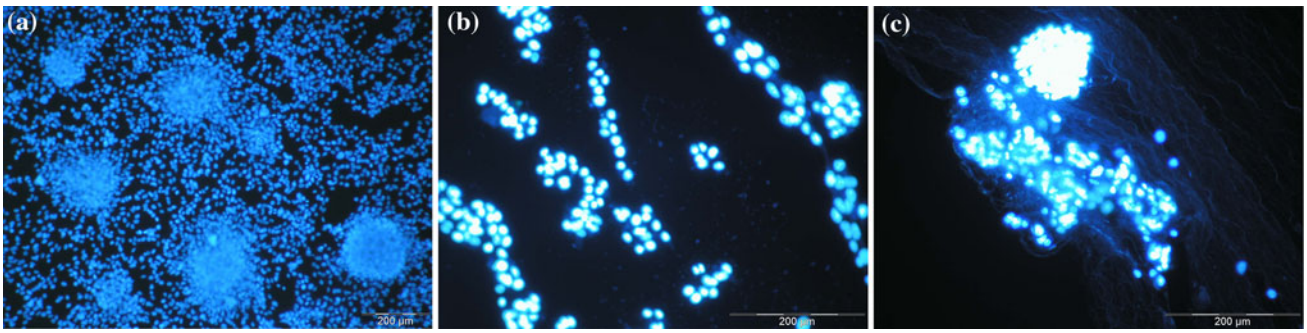

Fig. 16 DAPI dying of immortalized Schwann cells after 6 days of cultivation; glass slides **a** without fibers, **b** PEO without PEN, **c** PEN fibers

morphology on the three surfaces was considerably different. On the glass slides without fibers the cells showed a random cell growth and cell clusters. On the glass slides, coated with fibers, a cell growth in direction of the fibers was noticed. Particularly the cells on the PEN fibers grew in straight lines along the fiber.

The cell nuclei were stained with DAPI. Therefore the cells were fixed with ethanol. On the images (Figs. 15, 16) it can be seen that the fibers with cells detached from the glass slides. Therefore no statement about the cell density on the substrates can be made. But you can see better than in the phase-contrast pictures, how the cells grow along the detached fibers.

The viability of the cells was determined with a MTT assay, whereas the fibers also partly detached from the glass slides, thus the presented results in Fig. 17 can be affected by this problem. The viability of the cells on the glass slides without fibers is higher than on the coated slides. The viability of the cells is reduced with PEO fibers of about 26% and with PEN fibers of 22% in comparison to the pure glass slides. The results are based only on one data record, thus the results are statistically unsecured.

In summary the immortalized Schwann cells were less viable on the fibers than on the pure glass slide. The phase contrast images and the DAPI dying showed a cell growth

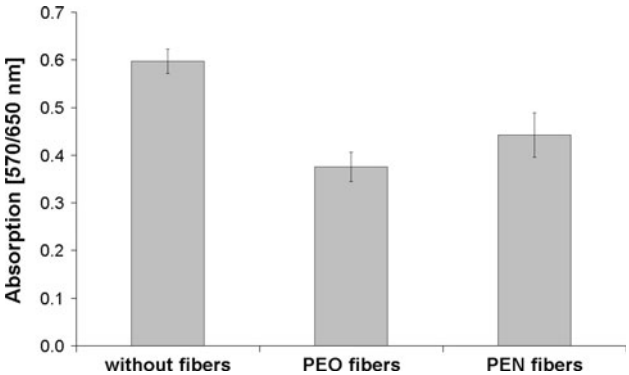

Fig. 17 MTT assay of immortalized Schwann cells after 6 days of cultivation; glass slides **a** without fibers, **b** PEO without PEN, **c** PEN fibers

in direction of the fibers. Particularly on the PEN fibers the cells grew towards the fiber direction.

4 Conclusion

In conclusion, a method to fabricate fiber scaffolds of PSA was developed. Therefore a binary system with PEO was used to stabilize the electrospinning process and to increase the mechanical stability of the electrospun fiber scaffolds.

Another advantage of the binary system is the economical handling of PSA, thus the production of this material is low cost.

To optimize the fiber scaffolds and to ensure the controlled variation of parameters in future works, the influence and interactions of process parameters on the morphology and the diameter of fibers were investigated by means of the PSA and PEO system. It was shown that with higher viscosities the fiber diameter can be increased. At higher conductivity the fiber morphology becomes smoother and with higher surface tension and conductivity the fiber diameter drops. By the variation of electrode geometries aligned fiber scaffolds could be obtained. A rotating drum will be used in the future, to improve the fiber density of the aligned scaffold.

The high water solubility of PSA could be minimized by preparing a photo-active derivative PEN, thus subsequent photochemical crosslinking was improved. In the future a photoactive, biodegradable copolymer instead of PEO will be used in combination with PEN to enhance the crosslinking and to create a biodegradable scaffold material.

In cell tests with the crosslinked fiber scaffolds a cell viability and a directed cell proliferation along the fibers were observed, which are promising results for future work to reach the goal of peripheral nerve regeneration by electrospun fibers scaffolds of PSA.

Acknowledgments This work was supported by DFG (Deutschen Forschungsgemeinschaft) and arose within the research group (FOR 548, "Polysialic acid: Towards the evaluation of a new bio-identical scaffold material"). Helpful discussions with Stefanie Böhm and Cornelia Kasper (Institut für Technische Chemie, Universität Hannover) are grateful acknowledged.

References

1. Kreis T, Vale R. Guidebook to the extracellular matrix, anchor, and adhesion proteins. 2nd ed. New York: Oxford University Press; 1999.
2. Norman JJ, Desai TA. Methods for fabrication of nanoscale topography for tissue engineering scaffolds. Ann Biomed Eng. 2006;34:89–101.
3. Li WJ, Laurencin CT, Caterson EJ, Tuan RS, Ko FK. Electrospun nanofibrous structure: a novel scaffold for tissue engineering. J Biomed Mater Res. 2002;60:613–21.
4. Sell S, Barnes C, Smith M, McClure M, Madutantakam P, Grant J, et al. Extracellular matrix regenerated: tissue engineering via electrospun biomimetric nanofibers. Polym Int. 2007;56:1349–60.
5. Sill TJ, von Recum HA. Electro spinning: applications in drug delivery and tissue engineering. Biomaterials. 2008;29:1989–2006.
6. van Blitterswijk C. Tissue engineering. 1st ed. London: Elsevier; 2008.
7. Evans GRD. Peripheral nerve injury: a review and approach to tissue engineered constructs. Anat Rec. 2001;263:396–404.
8. Schnell E, Klinkhammer K, Balzer S, Brook G, Klee D, Dalton P, et al. Guidance of glial cell migration and axonal growth on electrospun nanofibers of poly-epsilon-caprolactone and a collagen/poly-epsilon-caprolactone blend. Biomaterials. 2007;28:3012–25.
9. Yang F, Murugan R, Wang S, Ramakrishna S. Electrospinning of nano/micro scale poly(L-lactic acid) aligned fibers and their potential in neural tissue engineering. Biomaterials. 2005;26:2603–10.
10. Bini TB, Gao S, Tan TC, Wang S, Lim A, Hai LB, et al. Electrospun poly(L-lactide-*co*-glycolide) biodegradable polymer nanofibre tubes for peripheral nerve regeneration. Nanotechnology. 2004;15:1459–64.
11. Jungnick J, Brämera C, Bronzlika P, Lipokatic-Takacsa E, Weinhold B, Gerardy-Schahn R, et al. Level and localization of polysialic acid is critical for early peripheral nerve regeneration. Mol Cell Neurosci. 2009;40:374–81.
12. Senkov O, Sun M, Weinhold B, Gerardy-Schahn R, Schachner M, Dityatev A. Polysialylated neural cell adhesion molecule is involved in induction of long-term potentiation and memory acquisition and consolidation in a fear-conditioning paradigm. J Neurosci. 2006;36:10888–98.
13. Brusés JL, Rutishauser U. Roles, regulation, and mechanism of polysialic acid function during neural development. Biochimie. 2001;83:635–43.
14. Seidenfaden R, Krauter A, Schertzinger F, Gerardy-Schahn R, Hildebrandt H. Polysialic acid directs tumor cell growth by controlling heterophilic neural cell adhesion molecule interactions. Mol Cell Biol. 2003;23:5908–18.
15. Doycheva M, Petrova E, Stamenova R, Tsvetanov C, Riess G. UV-induced cross-linking of poly(ethylene oxide) in aqueous solution. Macromol Mater Eng. 2004;289:676–80.
16. Li D, Xia Y. Electrospinning of nanofibers: reinventing the wheel? Adv Mater. 2004;16:1151–70.
17. Burger C, Hsiao BS, Chu B. Nanofibrous materials and their applications. Annu Rev Mater Res. 2006;36:333–68.
18. Teo WE, Ramakrishna S. A review on electrospinning design and nanofibre assemblies. Nanotechnology. 2006;17:R89–106.
19. Shenoy SL, Bates WD, Frisch HL, Wnek GE. Role of chain entanglements on fiber formation during electrospinning of polymer solutions: good solvent, non-specific polymer–polymer interaction limit. Polymer. 2005;46:3372–84.
20. Reneker DH, Yarin AL, Fong H, Koombhongse S. Bending instability of electrically charged liquid jets of polymer solutions in electrospinning. J Appl Phys. 2000;87:4531–47.
21. Fong H, Chun I, Reneker DH. Beaded nanofibers formed during electrospinning. Polymer. 1999;40:4585–92.
22. Taylor G. Disintegration of water drops in electric field. Proc R Soc Lond. 1964;280:383–97.
23. Wang YK, Yong T, Ramakrishna S. Nanofibres and their influence on cells for tissue regeneration. Aust J Chem. 2005;58:704–12.
24. Li D, Wang Y, Xia Y. Electrospinning of polymeric and ceramic nanofibers as uniaxially aligned arrays. Nano Lett. 2003;3:1167–71.